

# Satellite self-damping Solar Array Deployment Mechanism design and simulation

Amir M. Wagih

Satellite structure dept., Space Technology  
Center  
STC, Cairo, 11838, Egypt

Ali El-tatawy

Satellite structure dept., Space Technology  
Center  
STC, Cairo, 11838, Egypt

**Abstract**—In this paper, a detailed design and simulation process of solar array deployment mechanism (SADM) for a large remote sensing satellite is presented. The mechanism is composed of three main assemblies; i) hinge assembly with torsion springs responsible for the mechanism rotation, and solar panel stoppage at the end of deployment stroke, ii) latch assembly to prevent reversed solar panel motion after deployment, iii) sensor assembly to measure the deployment angle. During torsion spring design, it was obvious that the final deployment moment is much lower than the initial deployment moment (i.e., self-damping) because of solar panel high inertia and latch friction with rotating part. Consequently, no braking mechanism is required and a simpler SADM design is achieved. A high-fidelity FE model is developed and mathematically verified for simulation process. SADM natural frequency and corresponding mode shape is extracted during modal analysis and results are compared to spacecraft natural frequency. A static analysis for SADM under input loading conditions during launch by Dnepr, Kosmos-3M, and Soyuz-U; and transportation by train, airplane, and car, is introduced. SADM frequency response and structure integrity are checked by harmonic analysis under launching loads. Due to the criticality of stoppage stage and the expected high collision impact for such large solar panel, an explicit dynamics analysis is carried out to ensure SADM safety. For large satellites with long lifetime periods, a fatigue failure is possible at solar panel root section under the effect of attitude control equipment operation. An in-orbit fatigue analysis is implemented on SADM and solar panel connection section using guidance and navigation load spectrum during satellite lifetime operation

**Keywords;** solar array deployment mechanism, satellite simulation.

## I. INTRODUCTION

A space mechanism commonly consists of the mechanical parts such as gears, springs, linkages, dampers, latches, cams which are assembled and worked together to achieve its operational goal [1]. A convenient approach to the study of spacecraft mechanisms is to divide them into two basic categories: i) One-shot devices; Are mechanisms required to function only once during the spacecraft

mission, and ii) Continuously operating devices: which include all those mechanisms that are required to operate continuously or intermittently. During transportation into space, a release device secures stowed deployable components such as antennas and solar arrays. In this study, solar array deployment mechanism (SADM), as an example of a one-shot device, is under the scope of work. Normally, solar arrays of considerable surface area are required to provide enough power for the safe payload functioning and for the computer and the communication systems. Solar panels are foldable to minimize size and space requirement on the launching vehicle. Self-actuated SADM utilizes the stored energy in a torsion spring to drive the solar arrays during the unfolding phase after orbital insertion. A stoppage element is essential in SADM to ensure the required deployment angle is achieved. In some cases, the motion has to be controlled by drag braking to reduce or eliminate the impact loading at the end of the stroke. Drag brake should be of minimum size and mass but can absorb and dissipate energy enough to make gradual deployment and smooth motion until the mechanism gets to rest at the end of the stroke, without shock loadings or reactions. however, in this study SADM smooth motion is fulfilled by: i) designing a torsion spring with moderate moment at the end of the deployment process, ii) using of a latch element to prevent the solar panel reverse motion after deployment, and iii) simulating the collision at the end of deployment to ensure SADM functionality

## Input Requirements and constraints

**Table 1 requirements and constraints [2]**

1) Solar panel rotation angle	= 90°
2) Time for deployment	= 6 -7 s
3) SADM mass budget	≤ 2Kg
4) SADM Overall envelope size	= 70 mm
5) The force necessary for operation of the micro-switch	= 0.1: 0.23 kgf [ref]
6) SADM natural frequency	>> 35 Hz

## II. MODEL

A detailed 3D model of SADM is shown in Fig.1. The developed model is composed of three main assemblies. 1) hinge assembly shown in Fig.2, 2) latch assembly shown Fig.3, and 3) sensor assembly shown in Fig.4.

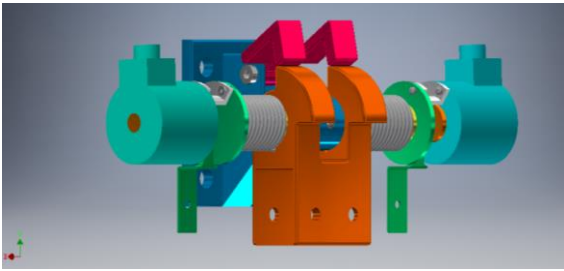


Fig. 1 SADM 3D model

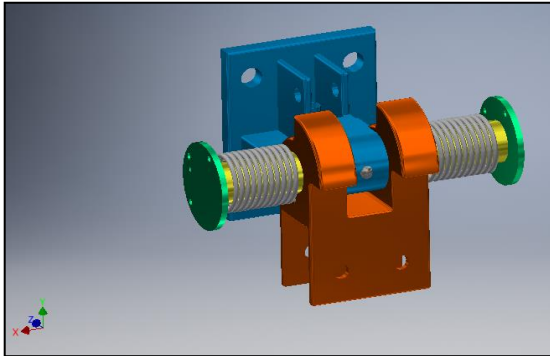


Fig. 2 hinge assembly

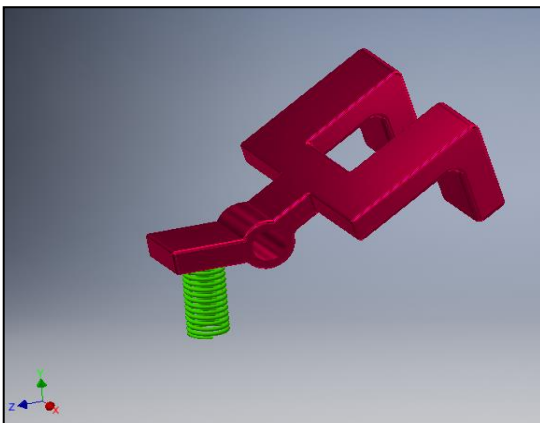


Fig. 3 latch assembly

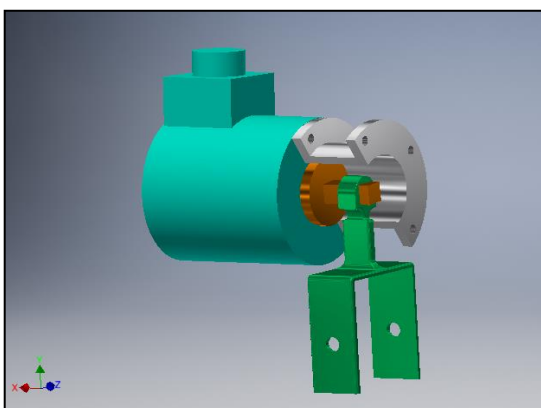


Fig. 4 sensor assembly

A. Torsion spring design

The final deployment moment of the spring ( $M_{f,dep}$ ):  

$$M_{f,dep} = 2M_{m,s} + \frac{M_c}{2} \quad (1)$$

$$M_{m,s} = F L \quad (2)$$

Where, F ranges from 0.98N to 2.25N (given by micro-switch supplier); for calculation we choose maximum force  $F=2.25N$ . The normal distance of the arm of force to the button of micro switch ( $L = 0.03m$ ). Each SADM has 2 micro switches ( $2M_{m,s} = 135.3 N.mm$ ), one switch is basic and the other is redundant.  $M_c$  is calculated experimentally by YOZHNOYE Design Office Dnepropetrovsk UKRAINE, which equals 700N.mm [3]. Taking into account possible discrepancies at carrying out of experiment, so a factor of stock  $T_o = 1.3$  is used [1];

$$M_c = (0.07) (T_o) = 892.4/2 = 446.2 N.mm \quad (3)$$

$$\text{Then } M_{f,dep} = 581.5 N.mm \quad (4)$$

The initial deployment moment necessary for accelerating of solar panel after release:

$$\sum M_{i,dep} = \frac{M_{inertia(S.A)}}{2} + M_{f,dep} + M_{fr} + M_{inertia(r.p)} \quad (5)$$

where:

$M_{inertia(S.A)}$  is solar array moment

$M_{inertia(r.p)}$  is rotating part moment

$M_{fr}$  is moment due to friction between latch and rotating part

$$\omega = 2\pi n = 2\pi (0.25/7) = 0.224 \text{ r/s} \quad (6)$$

$$\alpha = \frac{\omega}{t} = 0.0321 \text{ r/s}^2 \quad (7)$$

Where:

$\omega$  .... the angular velocity.

$t$  .... time of deployment.

The solar array outer dimensions are shown in fig.5. The solar array mass moment of inertia  $I_{S.A}$  is calculated:

$$I_{S.A} = I_z = \frac{m(a^2+b^2)}{12} = 9e5 \text{ kg. mm}^2 \quad (8)$$

$$M_{inertia(S.A)} = 294.2 N. mm \quad (9)$$

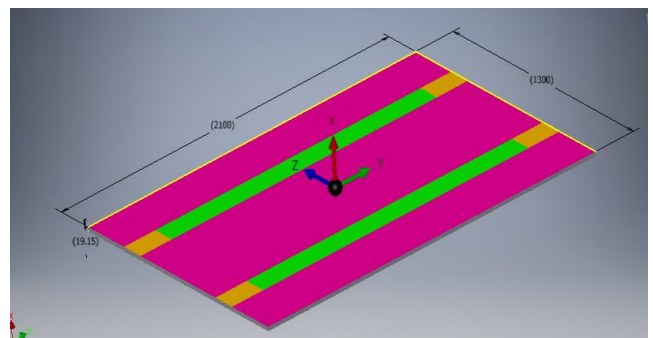


Fig. 5 solar panel dimensions

The rotating part mass moment of inertia of rotating part  $I_{r,p}$  is calculated:

$$I_{r,p} = 193e5 \text{ kg.mm}^2 \quad (10)$$

$$M_{inertia (r.p)} = 6.2 \text{ N.mm} \quad (11)$$

In order to calculate  $M_{fr}$ , the latch assembly compression spring is selected from commercial data sheet [ref.] such that to ensure the latch is loaded after locking at the end of deployment process (i.e.  $F_{i.1} = 14\text{N}$ ), where  $F_{i.1}$  is compression spring maximum load. Coefficient of friction for dry sliding aluminum = 1.4. then from fig.  $F_{i.2}$  is calculated around the latch axis of rotation. Then  $F_{fr}$  (friction force between latch and rotating part) is calculated as

$$F_{fr} = 6.58\text{N} \quad (12)$$

$$M_{fr} = F_{fr} * L_{fr} = 164.6\text{N.mm} \quad (13)$$

where:

$L_{fr}$  is the distance from rotating part center of rotation to the friction surface.

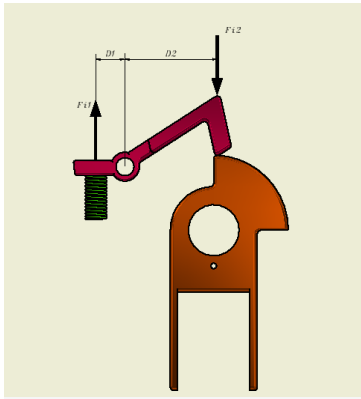


**Fig. 6 latch mechanism initial position**

by substituting in (5) then

$$M_{i.dep} = 893 \text{ N.mm} \quad (14)$$

taking into account the manufacturing deviations as  $\pm 10\%$ , then

$$M'_{i.dep} = 982.3 \text{ N.mm} \quad (15)$$

$$M'_{f.dep} = 639.65 \text{ N.mm} \quad (16)$$

In the proposed design, each SADM has two torsion springs, then initial moment and final moment per spring is:

$$M'_{i.dep/sp} = 491.15 \text{ N.mm} \quad (17)$$

$$M'_{f.dep/sp} = 319.82 \text{ N.mm} \quad (18)$$

Since the rotation angle is specified as:

$$(\phi_2 - \phi_1) = 90^\circ \quad (19)$$

Then rigidity of the spring C [6]:

$$C = \frac{M_2 - M'_{f.dep/sp}}{j_2 - j_1} = 1.68 \text{ N.mm/deg} \quad (20)$$

where: M2 is taken slightly lower than  $M'_{i.dep/sp}$  (i.e.  $M_2 = 471 \text{ N.mm}$ )

The operating twist angle of spring  $\phi_2$ :

$$\phi_2 = M_2 / C = 4.88 \text{ rad} \quad (21)$$

Rigidity of one coil of the spring  $C'$ :

$$C' = \frac{E * d^4}{64 * D * 57.3} = 19.4 \text{ N.mm/deg} \quad (22)$$

Number of working coils of the spring N:

$$N = C' / C = 11.5 \text{ turn} \quad (23)$$

Pitch of spring tt,

$$tt = f + d = 2\text{mm} \quad (24)$$

Length of a working part of the non-loaded spring

$$L_o = (tt * N) + d = 24.7\text{mm} \quad (25)$$

Mean diameter ( $D_1'$ ) of the spring after loaded with moment M2 is,

$$D_1' = \frac{D}{1 + \phi^2 / 2\pi n} = 17.49 \text{ mm} \quad (26)$$

Mandrel diameter ( $D_2'$ ) internal diameter after loaded:

$$D_2' = D_1' - d = 15.8 \text{ mm} \quad (27)$$

Increase in length of the spring after loading with moment M2:

$$\Delta L = \phi_2 * (D/2) \sin \alpha \quad (28)$$

$$\tan \alpha = d + f_3 / \pi * D \quad (29)$$

$$\alpha = 1.95^\circ \quad (30)$$

$$\Delta L = 1.55 \text{ mm} \quad (31)$$

Length of the spring after loading with moment M2,

$$L = L_o + \Delta L = 26.26 \text{ mm} \quad (32)$$

### B. Latching moment verification

The latching moment  $M_{latch}$  after deployment is checked to ensure latch is always loaded by compression spring in order to prevent solar panel reversible motion after latching as shown in fig. 7.  $F_{f1}$  = spring deflection \* spring rate = 10.35N, then:

$$M_{latch} = F_{f2} * D_{r2} = 106.75 \text{ N.mm} \quad (33)$$

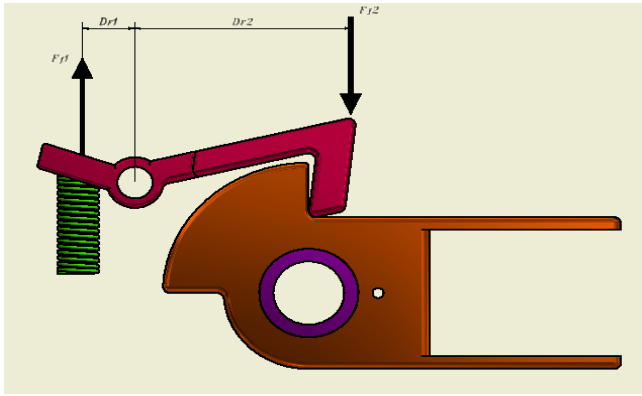


Fig. 7 latch mechanism final position

III. SIMULATION

A. FE model

A detailed FE model is developed using ANSYS workbench R19 [4] as shown in fig.8. FE model summary is described in table 2.

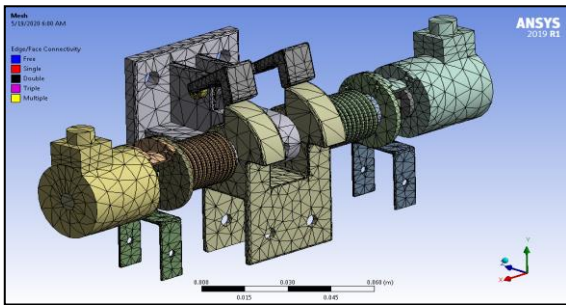


Fig. 8 SADM FE model

Table 2 FE model summary

Mass	Overall Dimensions	No of elements	No of nodes
0.275 Kg	189*65 mm	41466	131986

B. FE model verification

FE model is verified from mathematical perspective using three types of verifications: i) reaction check, to verify the consistency of boundary conditions, ii) Mass properties check, to compare the FE model w.r.t. the 3D model, and iii) Free-Free Modal Check to ensure that the free-free modal analysis will produce 6 rigid body modes (i.e., no missing contacts)

C. Static analysis

A static analysis is implemented on ANSYS R19 to get the stress distribution on SADM components [9] corresponding to each load event taking into account the probability of launch using Dnepr [1], or Kosmos-3M [2], or Soyuz-u [3]. Moreover, the satellite

transportation is planned to be by train, car, and IL-76. The most critical load events, determined according to the loading envelops shown in Fig.10 and Fig.11 [8] are: i) Aviation transportation (LC1), ii) 1st stage separation with Maximal longitudinal acceleration by Dnepr (LC2), and iii) Launch start by Soyuz (LC3).

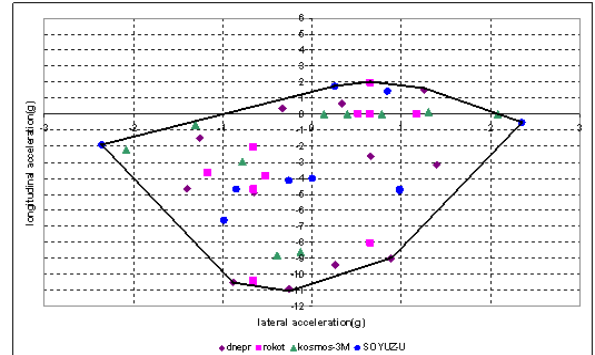


Fig. 9 Input load factors envelop during launch (lateral vs axial y)

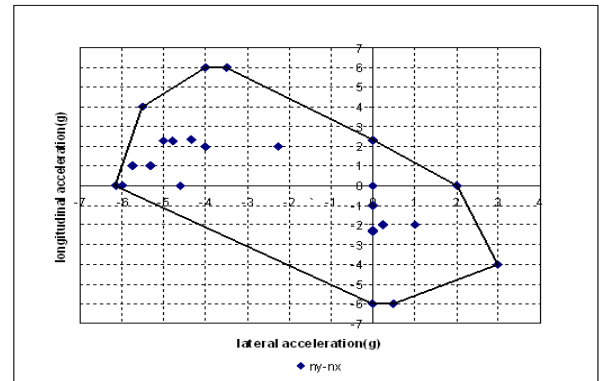


Fig. 10 Input load factors envelop during transportation (lateral y vs axial x)

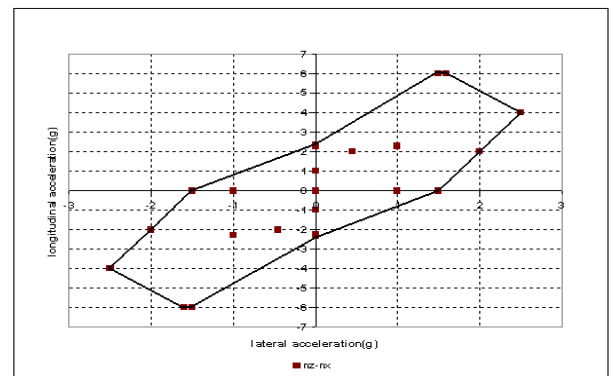


Fig. 11 Input load factors envelop during transportation (lateral z vs axial x)

These envelops were calculated from the input load factors for all the load cases as an initial indication of the worst load cases [5]. It is clear from these envelops that the above load cases are located on envelops' boundaries. The stress distribution on SADM components corresponding to LC1 is shown in fig. 12 for illustration. The strength margin values on

each component of SADM corresponding to each load case is shown in table 3.

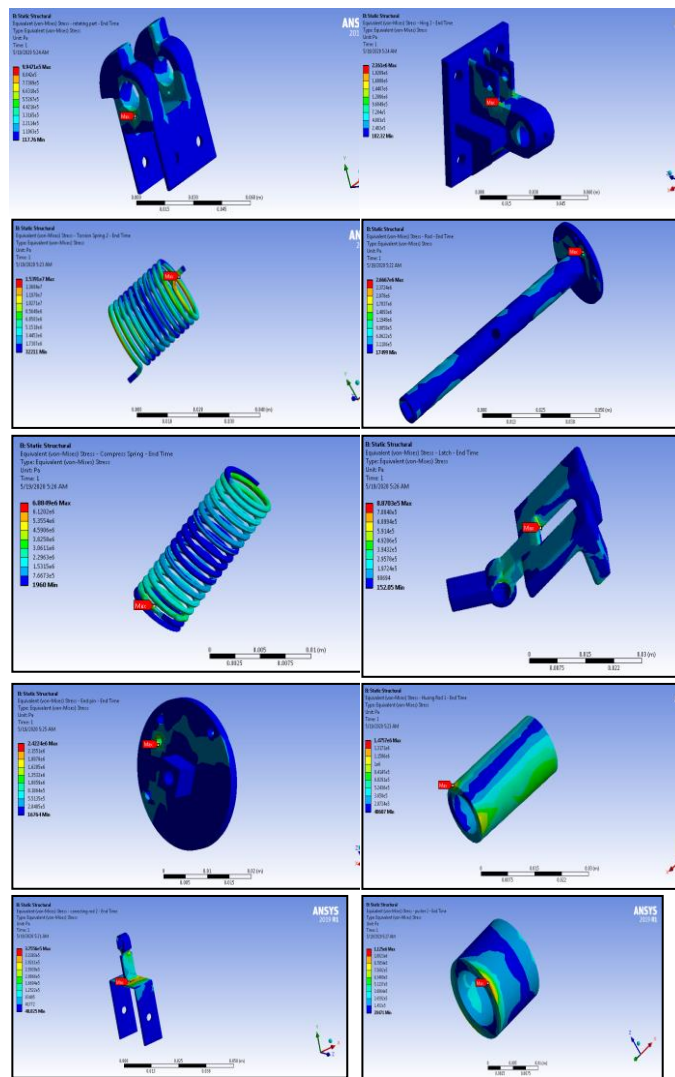


Fig. 12 SADM Stress distribution due to LC1

Table 3 static analysis strength margins value for each load case

SADM component	Strength Margin due to LC1	Strength Margin due to LC2	Strength Margin due to LC3
R.Part	249	362	181
Hinge	114.8	332	696
T.Spring	18	43	19
Rod	93	394	175
C.Spring	40	96	550
Latch	279.6	824	687
Connecting Rod	660	352	203
End Rod	102	285	270
Housing Rod	168	493	238

#### D. Modal analysis

The main purpose of this analysis is to extract the dynamic characteristics of SADM and ensure that first effective mode shape is much higher than satellite natural frequency (35 Hz) to avoid resonance [10], [11]. During analysis, results showed that SADM first natural frequency is equal to 140 Hz as shown in table 4.

Table 4 SADM natural frequencies & mode shapes

Mode#	Mode shape	Natural freq.(Hz)
1		140
2		144
3		193

#### E. Harmonic analysis

A harmonic analysis is used to check structure integrity & determine the response under a harmonic loading at a given frequency [12]. During harmonic analysis the launch case is considered as the most critical load event. Table 5, represents launching conditions by any of the four launchers mentioned before in the static analysis. The stress distribution is analyzed for each SADM and strength margins under harmonic loading is calculated as shown in table 6. Frequency response results are still in progress.

Table 5 equivalent harmonic loads during launch

Vibration direction	Frequency band, Hz								
	5-10	10-15	15-20	20-50	50-100	100-200	200-500	500-1000	1000-2000
	Amplitude of vibration acceleration, g								
Y	0.8	0.8-1.0	1.0-1.2	1.0-1.7	1.7-2.5	2.5-4.5	4.5-8.0	8.0	8.0
X, Z	0.5	0.5-1.0	1.0-0.5	1.0-1.7	1.7-2.5	2.5-4.5	4.5-8.0	8.0	8.0

**Table 6 harmonic analysis strength margin values**

SADM component	Strength Margin due to harmonic load
R.Part	20
Hinge	89
T.Spring	16
Rod	17
C.Spring	84.5
Latch	22
Connecting Rod	16
End Rod	51
Housing Rod	31

**F. Explicit dynamic analysis**

A separate simulation is held to account for the collision force that took place at the end of deployment stroke between the rotating part and the stoppage element. Due to the fact that solar panel is considerably large (i.e., high inertia), the collision can be quite critical to SADM design. During analysis, solar panel mass is added as lumped mass to include solar panel inertia force. An animated simulation results are shown as three consecutive frames in the following fig. 13, using explicit dynamic analysis tool in ANSYS 19 R1. Stress results showed that the impact force can cause no failure to SADM. Further calculations are in progress in which the solar panel FE model is inserted to make the simulation more realistic.

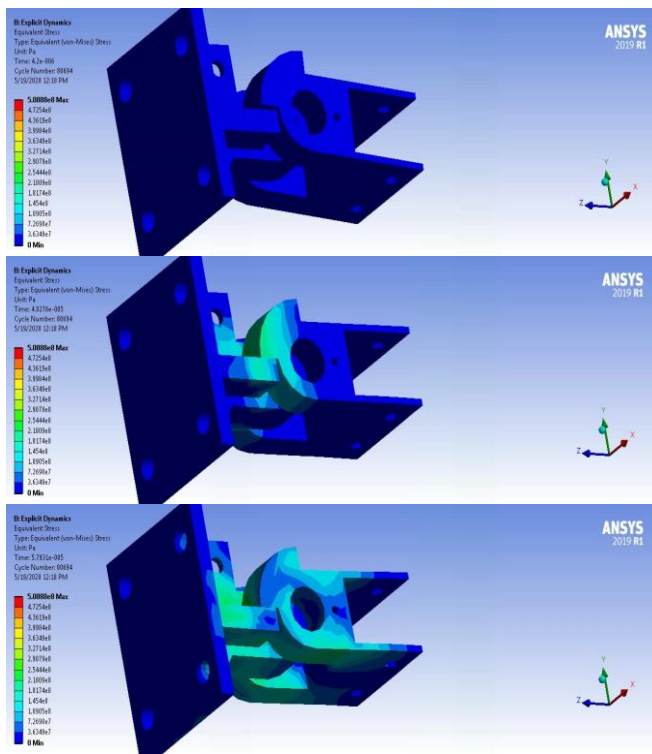


**Fig. 13 a) represents simulation frame 1 (pre-collision), b) represents simulation frame 2 (collision), c) represents simulation frame 3 (post-collision)**

**G. In-orbit fatigue analysis**

In orbit, the spacecraft uses special thrusters (rocket engines) and other aides (flywheels) to control its attitude and make orbit correction. An attitude control system rotates a spacecraft to point its sensors at their targets. It is possible to limit structural response by controlling the shape of acceleration time history for rotation maneuver. It is frequently used fast rotation named “forward-to-back”. It is implemented by firing a pair of thrusters in a short burst to apply a pure moment and then immediately firing another pair to introduce a moment in opposite direction. If this firing (impulse) period coincides with the period of natural frequency of any component, then such event is named impulse resonance. An approach, based on assessment of low and large cyclic fatigue and subsequent experimental (testing) validation of the required structure life using a generalized load spectrum, is used in this study. In this approach the modified Palmgren-Miner’s method [ref] is applied. The cumulative fatigue damage  $D_{fat}$ . is determined by equation:

$$D_{fat} = SF^k (\sum_{i=1}^k n_i/N_i) \quad (D \leq 1) \quad (34)$$

Where:

k – is the number of loading increments.

$n_i$  – is the predicted number of loading cycles at increment i.

$N_i$  – is the allowable (maximum) number of cycles at increment I from the appropriate S- N curve.

SF – is a scatter factor. It is introduced to account for variability in crack growth rates (usually we use SF equal 4 for testing and equal 10 for calculations).

The cumulative fatigue damage  $D_{fat}$ . is an indication of the percentage of the structure life which will be consumed under this fatigue loading (it should be less than or equal 1 not more). The values of k and  $n_i$  are determined by using the load spectrum for complete service life, which includes all significant loading events as shown in table 7. The S-N curve is a material characteristic, so that there should be an experimental S-N curve for the solar panel because this panel is composed of several materials with different properties. It should be noticed that in this stage time line diagram (load spectrum) of thrusters and flywheels operation in all modes is required as an input data from the guidance and navigation team. In order to implement this analysis, the values of the internal loads (moment, shear force and axial force) as shown in Table 7 are used as an input data. In this table the limit values of internal forces and moments at the root section of solar panel, and the corresponding operational number of load cycles are given for 4 modes of operation (load events). Solar panel is considered as the most critical structure element which will be affected by the load events during on-orbit operation phase due to its large surface area, small thickness and low mass. Due to the fact that solar panel has fixed-free boundary

conditions, the connection section between SADM rotating part and solar panel (i.e., root section) is considered most critical cross section as shown in fig.14. Stresses at the root section for each load event are calculated as shown in **Error! Reference source not found.** By extracting  $n_i$  value corresponding to each event stress value from the material S-N curve, and substituting in cumulative fatigue damage D equation, we get  $D_{fat.}$  approximately equals zero (i.e., no damage).

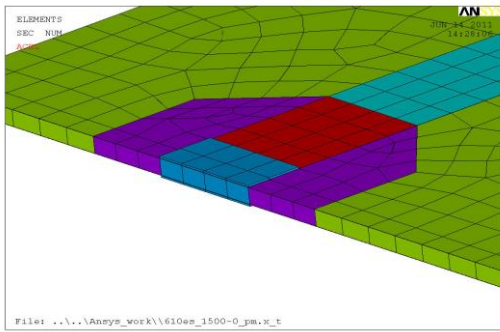


Fig. 14 SADM- solar panel root section

Table 7 internal loads and load cycles in the solar panel root section

Load event	limit value of the internal loads in the SA root section				Operational number of load cycles
	$\pm N $ (N)	Q, (N)	$\pm M_Y $ (N.mm)	M, (N.mm)	
Event 1	0.78	3.50	300	8800	$1.4 \times 10^4$
Event 2	0.46	1.85	200	4350	$1.2 \times 10^5$
Event 3	0.15	0.41	80	1020	$1.6 \times 10^6$
Event 4	0.01	0.03	50	230	$4.5 \times 10^7$

Notes

- 1.Event 1 represents insertion to the designated orbit.
- 2.Event 2 represents the orbit correction.
- 3.Event 3 represents the cancellation of angular velocities.
- 4.Event 4 represents loading and unloading flywheels.

Table 8 max. stress corresponding to each load event

Load event	maximum stress value (Pa)
Event 1	0.138 E7
Event 2	0.69 E6
Event 3	0.165 E6
Event 4	0.415 E5

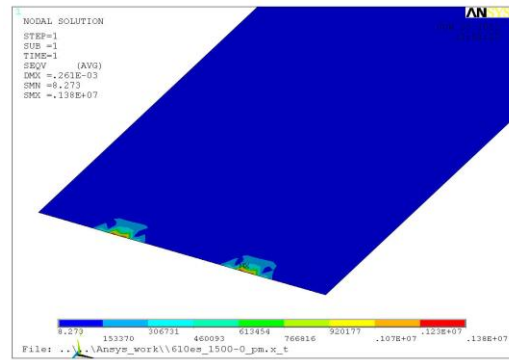


Fig. 15 max. stress corresponding to 1<sup>st</sup> load event

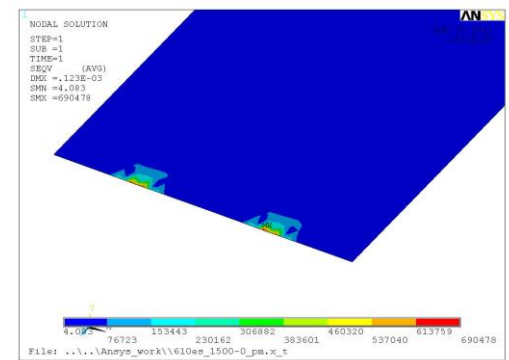


Fig. 16 max. stress corresponding to 2<sup>nd</sup> load event

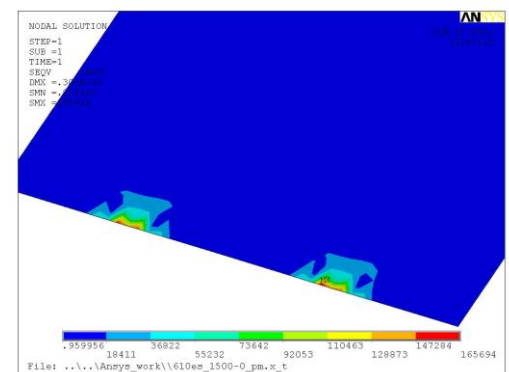


Fig. 17 max. stress corresponding to 3<sup>rd</sup> load event

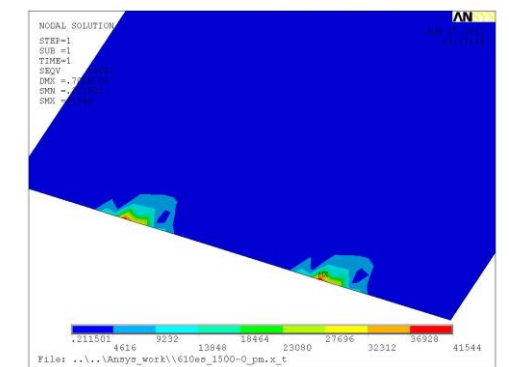


Fig. 18 max. stress corresponding to 4<sup>th</sup> load event

#### IV. CONCLUSION

This work has proposed a detailed design and simulation of SADM for large remote sensing satellite. Normally a smooth deployment process is achieved by using a braking mechanism or electric motors to prevent collision impact at the end of deployment stroke, which requires a more complicated design. The design of the torsion spring showed that the final deployment moment is much lower (35%) than the initial moment depending on large solar panel inertia and the friction imposed between the latch part and rotating part. An explicit dynamic analysis is carried out to simulate the collision impact and results showed that SADM is capable to withstand such impact force. As a result, the proposed SADM is considered as a self-damping mechanism and no braking or motion control is required. SADM is considered safe under static loading during launch BY either Dnepr, or Kosmos-3M, or Soyuz-U and transportation by airplane, car, and train. However static analysis strength margin results are considerably high indicating an over design case. The natural frequency of SADM is calculated (140Hz) and happens to be much higher than satellite natural frequency (35 Hz). Harmonic analysis was calculated during launch phase throughout low frequency and high frequency domains (5Hz-2000Hz) and results showed that SADM integrity is safe under dynamic loads. Moreover, the cumulative damage factor result showed that no damage is expected at solar panel connection with SADM during in-orbit fatigue analysis. The latch mechanism compression spring can be selected with different spring load to change the friction moment, consecutively changing initial deployment moment. Finally, it is clear that the proposed SADM design is quite simple, reliable (self-damping), redundant (two sensors, and two micro-switches), and easy to manufacture.

#### REFERENCES

- [1] M. G. El-Sherbiny, A. Khattab, M.K. Kassab. Design of the Deployment Mechanism of Solar Array on a Small Satellite. American Journal of Mechanical Engineering. 2013; 1(3):66-72. doi: 10.12691/ajme-1-3-2.
- [2] Wagih, A. M., Hegazy M., and Kamel M. "Pre-testing analysis of large remote sensing satellite's structure." AIAA SPACE 2016. 2016.
- [3] Fufa, B.; Zaho, C.; and Wensheag, M.; "Modeling and Simulation of Satellite Solar Panel Deployment and Locking" Information Technology Journal 9 (3): pp. 600-604, 2010.
- [4] ANSYS, Inc. Release 11.0 Documentation for ANSYS.
- [5] Kosmotras. "Dnepr User's Guide." manual, 2001.
- [6] Polyot, PO. "kosmos 3M User's Manual." Manual, 2001.
- [7] Starsem. "Soyuz User's Manual." manual, 2001.
- [8] Wagih, A. M., Hegaze, M., and Kamel, M. "Satellite FE model validation for coupled load analysis using conventional and enhanced correlation criteria." AIAA SPACE and Astronautics Forum and Exposition.2017.
- [9] Sadkin, Y. "Spacecraft Quasi-Static Test Performed on a Shaker." 5th International Symposium on Environmental Testing for Space Programmes. 2004. 203-208.
- [10] Shibabrat N., Wrik M., "Experimental Modal Testing for Estimating the Dynamic Properties of a Cantilever Beam" , Department of Civil Engineering , Jadavpur University, Kolkato700 032.
- [11] Heylen W., Lammens S., Sas P.: Modal Analysis Theory and Testing, Katholieke Universiteit, Leuven, 1997.
- [12] Bart B. Wim H. and Jan D.; "Modern Solutions for Ground Vibration Testing of Large Aircraft"; LMS International, Leuven, Belgium, SAE International Journal of Aerospace, April, 2009, Vol. 1, No. 1, pp. 732-742, 2009.